CHAPTER 5

Effect of intercalation and vertical hetero-structure Silicene/$SnSe_2$ over the electronic properties of Silicene

5.1 Introduction

Another popular two-dimensional material, silicene confined form of silicon had been predicted theoretically by Takeda et al. in 1994[1] even before the isolation of graphene. However, unlike graphene, planar silicene was found unstable and difficult to synthesize. In 2009, theoretically it was shown that the silicene is dynamically stable with low buckled geometry at temperature T=1000 K.[2] However, experimentally, it is challenging to synthesize buckled silicene, as it does not descents like graphene, transition metal dichalcogenides (TMDs) and other two-dimensional materials while mechanically stripping from its bulk phase.[3,4] In 2012, silicene was artificially synthesized in a suite under high vacuum with no parent bulk crystal unlike graphene.[5] Silicene consists silicon atoms arranged in a honeycomb lattice structure similar to graphene, with buckling height of 0.44 Å. Silicene exhibits semi-metallic nature besides having sp^2-sp^3 hybridization preserving the Dirac cone at the high symmetry point '**K**' of the Brillouin zone (BZ).[6,7] The silicene monolayer like germanene and stanene is not found naturally and need to be synthesized. The silicene monolayer and its multi-layered configuration have been grown on several metal substrates such as Ag(111), Ir(111) and $ZrB_2(0001)$ by molecular-beam epitaxial (MBE) method,[8–13] and have been explored for various applications such as valleytronics, spintronics, superconductivity, field effect transistor (FET), tunnelling FET, thermoelectric effect, gas sensor etc.[7,14–20] The selection of substrate is an important factor for the fabrication of materials with desired properties, as for silicene, it is observed that the Dirac cone vanishes due to change in π bonding arising from strong interaction between substrate and silicene.[11,21,22] In case of graphene, it is found that the graphene losses its Dirac cone while chemisorbed on surface of transition metals Ni, Co, Ti and Pd due to strong hybridization between d-state of transition metal and p_z state of graphene whereas, for Al, Cu, Ag and Pt substrates it preserves the Dirac cone due to weak interaction with the substrate material.[23–27]

Perseverance of Dirac cone is important for high speed field effect transistors[28] and band opening is necessary for electronic applications. However, the semi-metallic nature of pure silicene is a hindrance for its utilization in the electronic applications similar to graphene. To avoid strong interaction between substrate and silicene, and for opening the bandgap with preservation of Dirac cone, many semi-conducting and metal substrates have been tried. Quhe et al.[29] showed that the silicene acts as a p-type dopant for metal substrates such as Ir, Au, and Pt whereas, it serves as n-type dopant for Al, Cu and Mg substrates and a strong interaction between these substrates and silicene is found that ultimately leads to destruction of Dirac cone.[29] Many efforts have been devoted to preserve the Dirac cone, opening of band gap and maintaining the stability of low buckled silicene over strongly interacting substrates. Dirac cone of silicene can be well preserved due to weak interaction between substrates and silicene via vdW-type interaction but shows less possibility of low buckled silicene to be stable.[30–34] The low buckled silicene was found to be stable and favourable on semi-conducting substrates such as GaP, GaAs, ZnS, and ZnSe with loss of Dirac cone.[32,35] Regarding band gap opening, it was shown that the wide band gap semi-conductor substrates such as $Al_2O_3(0001)$, MoS_2, GaS, etc. can open the band gap of silicene.[36–38] Thus, stability is a major concern together with the band opening of silicene. The band opening of 170 meV is observed with GaS nanosheet having lattice mismatch of about 7.5 %.[37] This high magnitude of mismatch indicates a possibility of generating instability in hetero-structure. Therefore, the search of novel substrates which exhibit lower mismatch with low buckled (LB) silicene is essential. Previous studies show that the many metal dichalcogenides such as MoS_2, $MoTe_2$, WSe_2 and SnS_2 are potential substrates, as they possess less lattice mismatch with silicene and help in band opening.[39–43] Apart from these materials, $SnSe_2$ is a post-transition metal dichalcogenide that possesses both desired characteristics, low lattice mismatch and semi-conducting nature which motivates to analyse the properties of hetero-structure of silicene and $SnSe_2$. Literature survey reveals that the strong interaction between a Si/$PtSe_2$ hetero-structure can be made weaker with the incorporation of gas molecules such as CO_2, NO_2 and NH_3 due to their diffusion barriers.[44] Among these three gases, NH_3 shows good diffusion barrier between silicene and $PtSe_2$. Beside gas molecules, intercalation of different atoms such as alkali and halogen atoms between the hetero-layers has been utilized to tune the electronic properties of graphene nano ribbon staked over hexagonal boron nitride (h-BN) sheet with increasing their interlayer distance.[45]

In this work we have studied the electronic properties and stability of silicene over $SnSe_2$ monolayer (Si/$SnSe_2$) and the effect of intercalation of ammonia molecule (NH_3), chlorine (Cl) and phosphorous (P) on the electronic properties of Si/$SnSe_2$ hetero-structure. For application point view, we have studied CO sensing over individual monolayers and hetero-structured configuration.

5.2 Computational method

First-principles calculations were performed by using generalized gradient approximation (GGA)[46] under the frame work of the density functional theory (DFT)[47] implemented in Quantum Espresso simulation package.[48] The plane wave pseudo-potential method together with Perdew, Burke and Ernzerhof (PBE-GGA) type exchange-correlation functional has been utilized for solving many body Kohn-Sham equation.[46] The kinetic energy cut-off for plane-wave basis was set to 100 Ry for all considered systems following convergence test. The scheme of Monkhorst-Pack has been used to generate **k**-point mesh in the reciprocal space, where the Brillouin zone (BZ) integration was carried out using 9×9×1 **k**-points mesh.[49] For the structural optimization, the maximum force allowed on each atom was set to be less than 10^{-4} eV/Å which was found better for achieving ground state of the systems. In order to effectively describe the non-local and long-range nature of van der Waals (vdW) interaction in the layered materials, we have included long-range dispersive interactions with vdW interaction throughout the calculation and performed dispersion corrected density functional (DFT-D2)[50] calculations. Further, to analyze the stability of the hetero-structure Si/$SnSe_2$, we have calculated formation energy which is expressed as follows:

$$E_{form} = (E_{Si/SnSe_2} - E_{SnSe_2} - E_{Si})/\, N_{Si} \qquad (5.1)$$

Where, $E_{Si/SnSe_2}$, E_{Si}, and E_{SnSe_2} represent the total energies of the Si/$SnSe_2$ hetero-structure, isolated low buckled (LB) silicene, and isolated $SnSe_2$, respectively. N_{Si} is the number of Si atoms in the supercell of the hetero-structure. The cohesive energy per Si atom for silicene on monolayer $SnSe_2$ is calculated to know the possibility of synthesizing silicene over $SnSe_2$ hetero-structure, which is defined as under:

$$E_c = \mu_{Si} - (E_{Si/SnSe_2} - E_{SnSe_2})/ N_{Si} \tag{5.2}$$

Where, μ_{Si} is the chemical potential of Si (total energy of an isolated Si atom), $E_{Si/SnSe_2}$ and E_{SnSe_2} represent the total energies of the Si/$SnSe_2$ hetero-structure and isolated $SnSe_2$, respectively. We have calculated the binding energy of intercalated atoms or molecules between hetero-structure as it is essential to investigate the stability of hetero-structure after the intercalation using following expression:

$$E_b = E_{tot(x)} + E_{tot(Si/SnSe_2)} - E_{tot(Si/x/SnSe_2)} \tag{5.3}$$

Where, $E_{tot(x)}$ is total energy of intercalated atoms or molecules (x = P, Cl and NH_3), $E_{tot(Si/SnSe_2)}$ and $E_{tot(Si/x/SnSe_2)}$ represent the total energies of the $Si/SnSe_2$ hetero-structure and intercalated hetero-structure ($Si/x/SnSe_2$), respectively. We have also calculated the energy required to peel off silicene from the intercalated atoms or molecules adsorbed surface using following equation:

$$E_b = (E_{tot(Si)} + E_{tot(x/SnSe_2)} - E_{tot(Si/x/SnSe_2)})/ N_{Si} \tag{5.3}$$

Where, $E_{tot(x/SnSe_2)}$ is total energy of intercalated atom or molecule over $SnSe_2$.

5.3 Results and Discussion

5.3.1 Structural and electronic properties of silicene, $SnSe_2$ and Si/$SnSe_2$

Before the analysis of hetero-structure, we have individually optimized the 2x2 super cells of low buckled silicene (Si) and tin di-selenide ($SnSe_2$). We have found that the structural parameters and electronic band gap of both monolayers Si and $SnSe_2$ are in good agreement with previously reported data (listed in Table 5.1). The Table 5.1 depicts that the lattice mismatch between Si and $SnSe_2$ is about 0.48 % which is less than 1.8 %, therefore, lattice match model can be employed to have vertical hetero-structure made-up of silicene over $SnSe_2$ (Si/$SnSe_2$). Initially, inter-layer distance between both hetero-layers is kept as 2 Å with respect to selenide atoms, and about 15 Å of vacuum between two-periodic hetero-structure images to avoid interaction. The optimized geometry of Si/$SnSe_2$ hetero-structure is shown in Fig. 5.1, where, the interlayer distance between silence and selenide atoms at the end of optimization gets increased and was found to be 3.903 Å (as shown in Fig. 5.1(a)). The optimized lattice constants

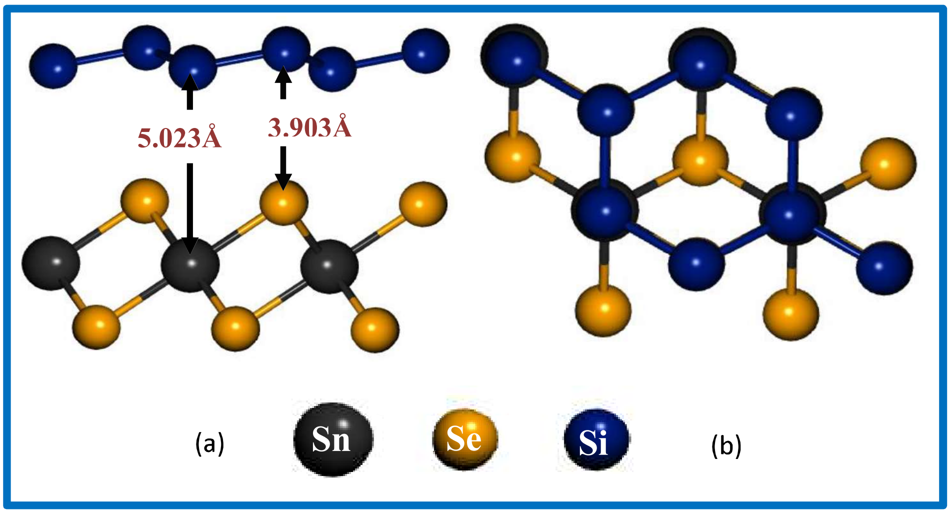

Figure 5.1: The optimized structure of hetero-structure Si/$SnSe_2$, (a) side view and (b) top view.

of 2x2 supercells of silicene (Si), SnSe$_2$ and hetero-structure Si/SnSe$_2$ are 7.6545 Å, 7.6924 Å and 7.6645 Å, respectively (see Table 5.1). We observed that the buckling height of silicene increases by 5.4 % as compared to the optimized free standing silicene (0.467 Å) in hetero-structured configuration due to the strong interaction between Si and SnSe$_2$ monolayers. It is interesting to note that the buckling height of silicene (hetero-structure) is 77 % lower as compared to high buckled silicene (2.146 Å).[10] The bulking height (h) of silicene can be co-related with the lattice mismatch between silicene and di-chalcogenide substrates. These results show that the lattice match (0.48 %) leads to lower buckling height (0.492 Å) which is in good agreement with previous observation.[40]

Fig. 5.2(a-c) represents the electronic band structure of silicene, SnSe$_2$ and hetero-structure along the high symmetry directions of the BZ, which clearly depicts that the silicene,

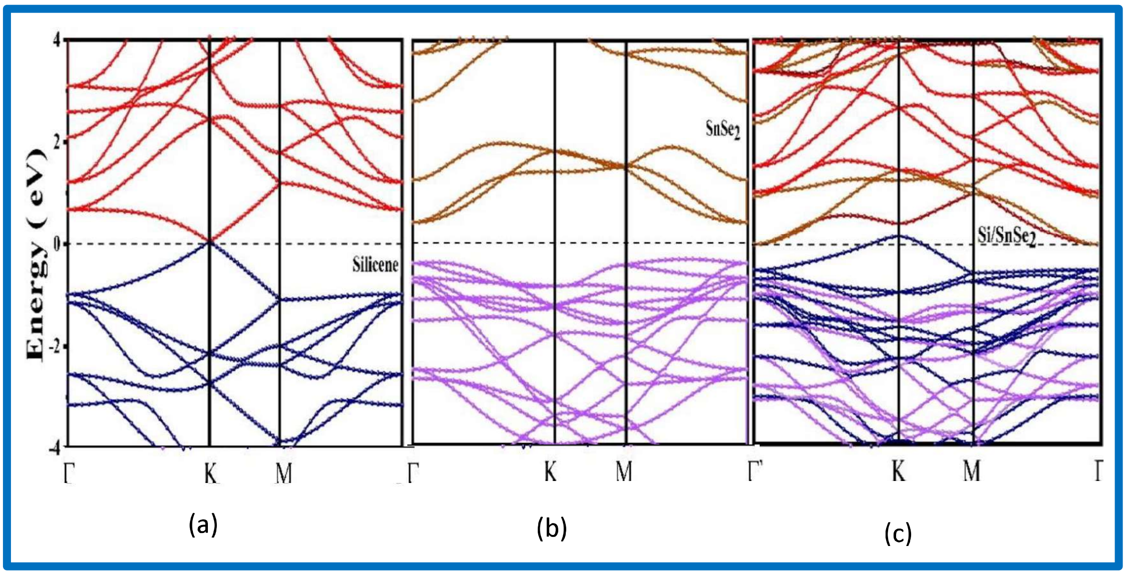

Figure 5.2: The electronic band structure of (a) silicene, (b) SnSe$_2$ and hetero-structure Si/SnSe$_2$; red (blue) and brown (violet) represents conduction bands (valance bands) of Silicene and SnSe$_2$ respectively.

SnSe$_2$ and hetero-structure have semi-metallic, semi-conducting with a band gap of 0.84 eV and metallic behavior, respectively.

The Dirac cone can be observed at **K**- point of the BZ (see Fig. 5.2(a)) for free standing silicene. It is also noticed that the degeneracy decreases along **K→M** direction for Si/SnSe$_2$. The band profiles of Si and Si/SnSe$_2$ hetero-structure are quite alike (as seen from red (conduction bands) and blue (valance bands) curves) in hetero-structure, except the bands at **Γ**-point of free-standing Si which do not show band gap whereas an opening of band gap at **K**-point of hetero-structure is observed which shifts towards conduction band side after crossing Fermi level. Moreover, this shifting increases the metallicity of hetero-structure as the maximum contribution to the conduction band is due to SnSe$_2$ of hetero-structure. The metallic nature of silicene seems to be originated due to the increment in the buckling height of silicene. These results are consistent with earlier study which states that for preserving semi-metallic nature of silicene, we need to reduce the buckling height that can be achieved by increasing in-plane lattice parameter of the di-chalcogenide substrate.[40] Similar pattern can be observed from total density

Table 5.1: Optimized lattice constant and electronic properties of 2x2 supercell silicene, SnSe2 and hetero-structure Si/SnSe2.

System	Lattice parameters (Å)	Band gap (eV)
Silicene (Si)	7.6545	0
SnSe$_2$	7.6924	0.84
Si/SnSe$_2$	7.6645	Metallic

states of $SnSe_2$, Si and Si/$SnSe_2$ hetero-structure as shown in Fig. 5.3(a). The metallic nature of Si/$SnSe_2$ is due to overlapping of density of states of silicene and $SnSe_2$ near the Fermi level. In order to have a deeper insight into electronic properties of hetero-structure at atomic level, we have calculated the partial density of states of Si/$SnSe_2$ hetero-structure (see Fig. 5.3(b)). The metallic nature of Si/$SnSe_2$ is mainly due to the overlapping of density of states of p-orbital of Si and Se with the s-orbital of Sn. We conclude that the strong interaction between $SnSe_2$ and silicene leads to metallic nature. Further, we have observed that the buckling height of silicene

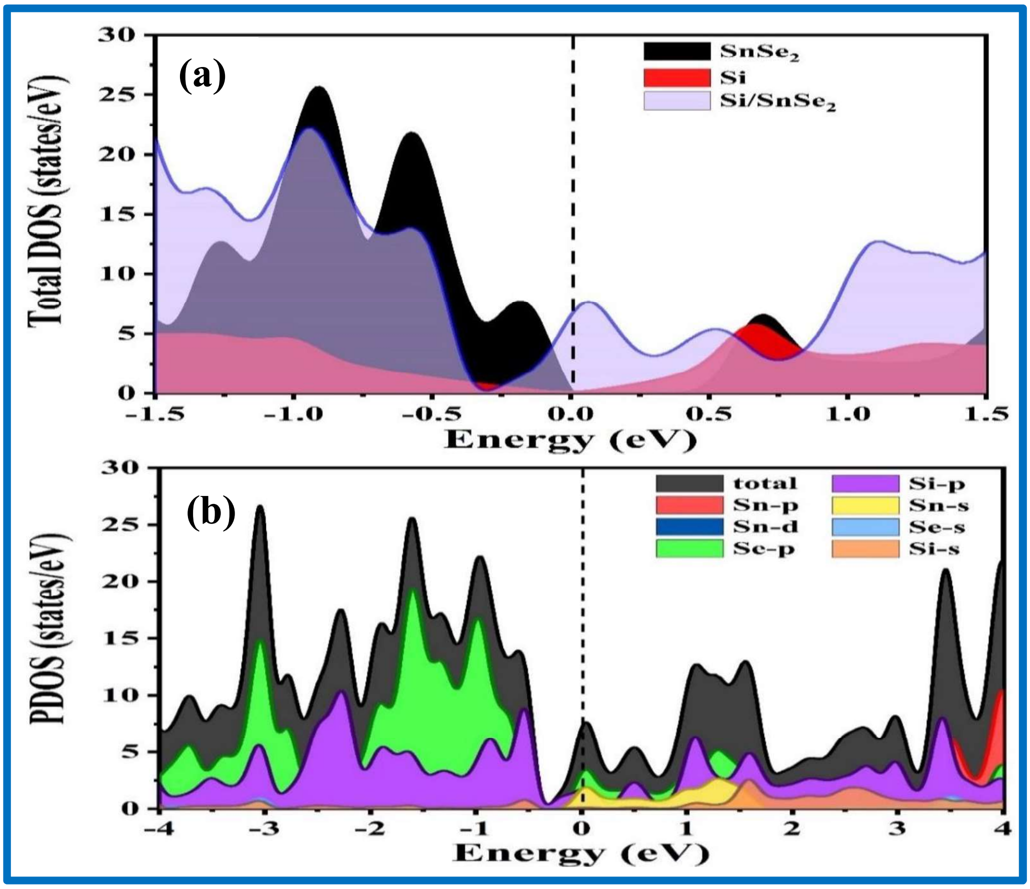

Figure 5.3: (a) Total density of states of $SnSe_2$, silicene and Si/$SnSe_2$ hetero-structure and (b)partial density of states of hetero-structure Si/$SnSe_2$.

layer is lower despite metallic nature. This result does not follow the previous observation that the electronic properties of silicene on different di-chalcogenide substrates depend upon buckling height. Our study suggests its dependency on the interaction between substrates and silicene monolayer.

The stability is one of the important factors for the potential application of any material. Therefore, we have calculated the formation energy of hetero-structure and found it to be -0.5449 eV which suggests that the formation of hetero-structure is an exothermic process and energetically favorable as compared to the semi-conducting substrates investigated previously which are −0.120 eV over MoS_2, −0.126 eV over GaS and −0.279 eV over $PtSe_2$, respectively.[36,37,44] The cohesive energy of hetero-structure is found to be 4.79 eV that is slightly higher than the free standing silicene (4.77 eV)[44] which indicates the possibility of growth of silicene over $SnSe_2$. The silicene over $SnSe_2$ is unavoidably metallic due to the strong interaction between Si and $SnSe_2$ which indicates it less suitability for electronic applications. However, we believe that the intercalation of p-type atoms (such as P and Cl) and NH_3 may lead to weak interaction with the epitaxial sheet and preserve its ideal LB structure as reported for hetero-structure Si/$PtSe_2$.[13]

5.3.2 Effect of intercalation over the Structural and electronic properties of Si/$SnSe_2$

Intercalation has been proved good enough to recover the Dirac cone which disappeared/distracted due to the strong interaction between the silicene and metal substrates and for the opening of band gap. We have intercalated NH_3 molecule, phosphorous (P) and chlorine (Cl) between the hetero-layers.

5.3.2.1 Structural and electronic properties of hetero-structure (Si/$SnSe_2$) with intercalated chlorine atom.

We have initially intercalated Cl atom at the hollow site of hetero-structure as shown in Fig. 5.4 (a) and, after relaxation, the Cl atom preferers to be at the edge site (see Fig. 5.4(b)) like in the case of graphene nanoribbon/h-BN stacked layer.[45] We have calculated binding energy using

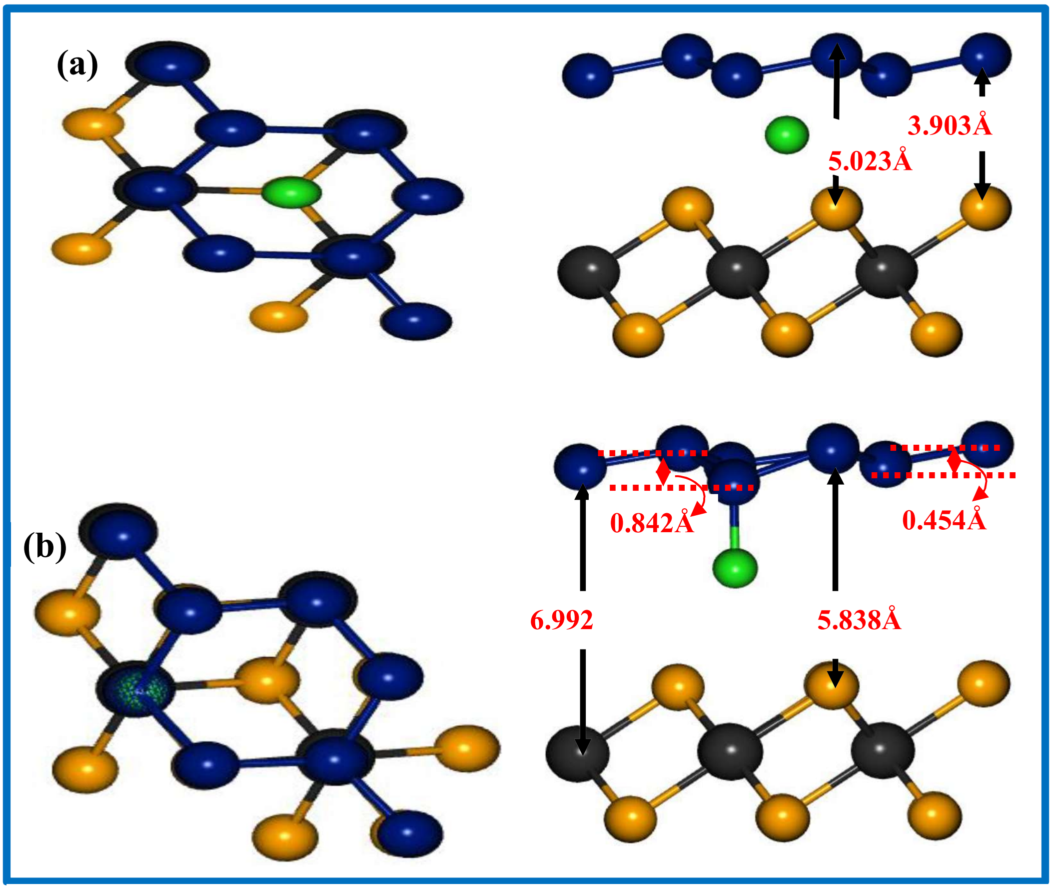

Figure 5.4*:* Top and side view of (a) initial and (b) optimized structure of Cl-intercalated hetero-structure Si/$SnSe_2$ respectively.

equation 5.2 to find the possibility of intercalation of Cl with hetero-structure. The positive (negative) value of binding energy shows the process as exothermic (endothermic). The binding energy of intercalated Cl atom is 3.05 eV which indicates that the process is exothermic and leads to a stable configuration. The interlayer distance between hetero-structure increases with intercalation of Cl atom. The increment of about 0.39 % and 0.49 % is observed in the distance between Si and Sn atoms (d_{Si-Sn}) and Si and Se atoms (d_{Si-Se}), respectively. The buckling height of Cl bonded Si atom increases (0.842 Å) with respect to pristine silicene (0.467 Å) and hetero-structure (0.492 Å) (See Fig. 5.4(b)). This can be attributed to the fact that the Cl atom strongly binds with Si atom of silicene. The strong interaction between atoms of Cl and silicene monolayer is due to strong electronegativity of Cl atom which tends to share electron with bonded silicene. This result suggests that intercalation has less probability of preserving Dirac cone or band opening of silicene even though the increment in the interlayer distance between hetero-structure, which weakens interaction between silicene and $SnSe_2$. To understand the above findings more clearly, we analyzed band structure, PDOS and charge-density. The band structure of intercalated Cl, clearly depicts its metallic nature by forming defect band near the Fermi level (see Fig. 5.5(a)) responsible for electron scattering. We have plotted the PDOS of Sn, Se and Si to investigate the contribution of atoms in electronic properties of Si/Cl/$SnSe_2$. We can clearly see that the overlapping of PDOS of bonded Si atom with Cl atom results in metallic nature of Si/Cl/$SnSe_2$. The formation of chemical bond between Cl and Si edge atoms of silicene monolayer leads to sp^3 hybridization in silicene.

Lowdin charge analysis has been carried out to study the charge transfer between constituent atoms. This analysis helps in finding charge transfer to atoms or molecules from metal substrates. The initial charges on silicene sheet, $SnSe_2$ and isolated Cl were 31.42 e, 104.03

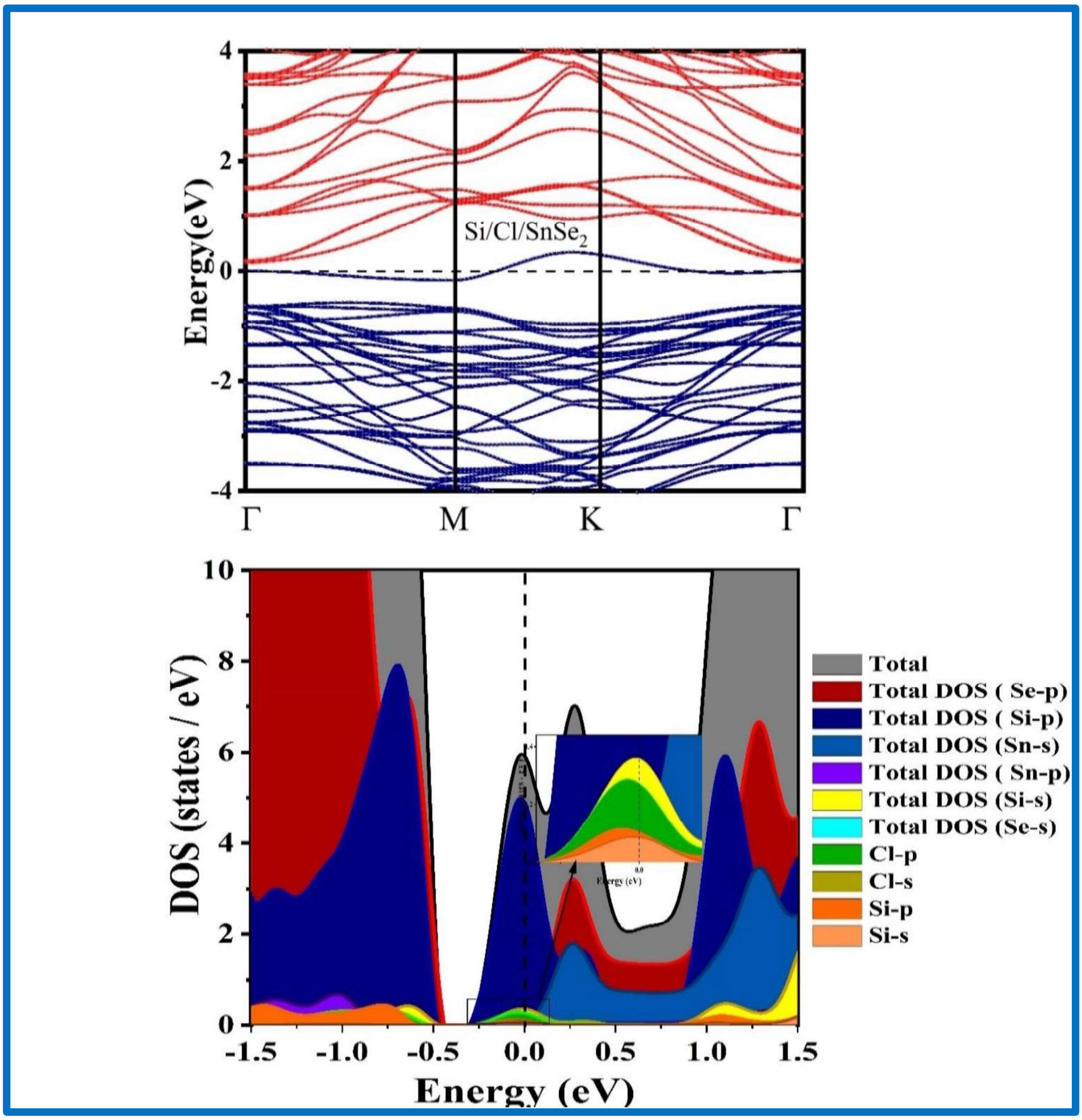

Figure 5.5*:* (a) The electronic band structure and (b) partial density of state (PDOS) of Cl-intercalated hetero-structure Si/$SnSe_2$.

e and 7 e, respectively. However, the intercalation of Cl atom between hetero-structure, the charge on silicene sheet decreases (0.65 %) while charge increases for Cl (3.4 %) and $SnSe_2$ (0.67 %). This means that the charge from silicene is transferred to Cl atoms followed by $SnSe_2$. To ensure the above results; the charge density plot is shown in Fig. 5.6. We draw similar conclusion from charge density plot where, chemically bonded Cl atom acquires more charge (surrounded by cyan color) as compared to Si atoms due to higher electronegativity of chlorine atom. The electron prefers to reside more towards chlorine side. The yellow region between hetero-structure near Cl and $SnSe_2$ shows less charge density between Cl and $SnSe_2$. These results are in good agreement with our Lowdin charge analysis. We observe that the intercalation of Cl atoms increases the interlayer distance between Si and $SnSe_2$ but it is not enough to weaken the interaction between them, as Cl interacts with silicene monolayer strongly. Therefore, we

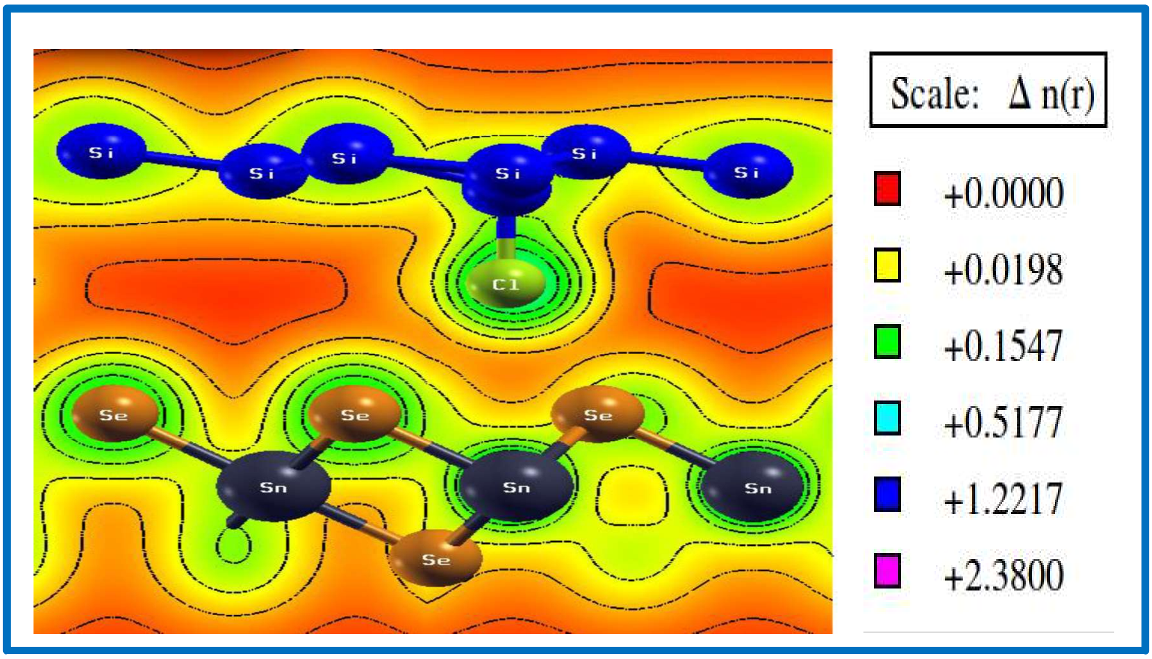

Figure 5.6: The charge density plot of Cl-intercalated Si/$SnSe_2$ hetero-structure.

need dopant that acquires charge from silicene and does not interact with $SnSe_2$. Another considered candidate for p-type dopant is phosphorous (P) which is lesser electronegativity as compared to chlorine (Cl).

5.3.2.2 Structural and electronic properties of (Si/$SnSe_2$) hetero-structure with intercalated phosphorous (P) atom

We placed phosphorus atom at the same position as chlorine atom. P atom prefers hollow site instead of edge position unlike Cl atom. The reason behind P atom preferring hollow site instead of edge position, is its valency and electronegativity. The intercalated Cl atom form bond with single edge Si atoms whereas, intercalated P atom forms chemical bond with nearby three Si atoms due to its three unpaired electrons in p-orbit of valence shell as shown in Fig.5.7. We observe that the bond formation between P and Si atoms of silicene sheet is a result of high electron negativity of phosphorous atom. It is interesting to note that the Si atom of silicene sheet form strong chemical bond with the Se atom of $SnSe_2$. This strong interaction makes

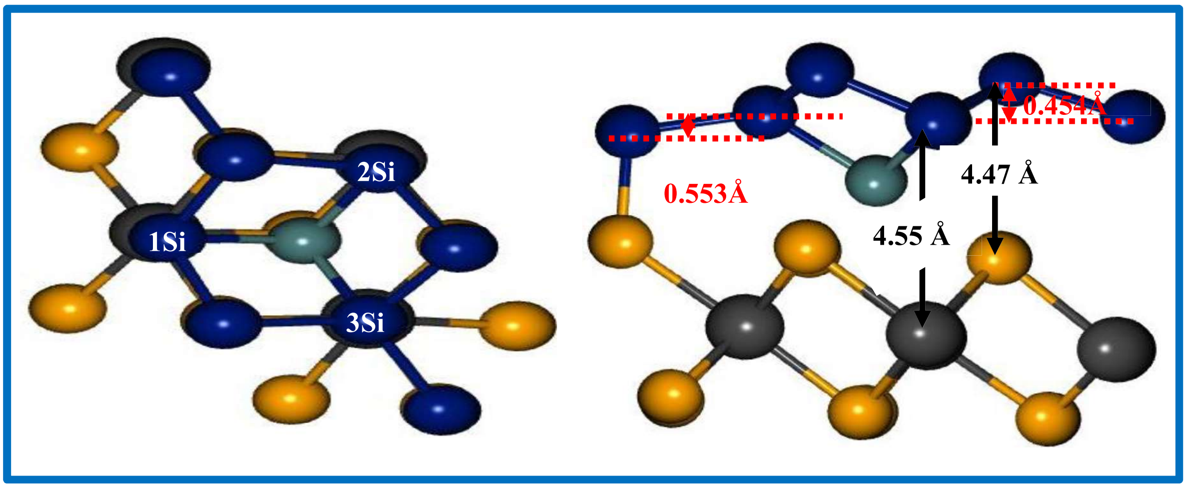

Figure 5.7*:* Top and side view of optimized structure of P-intercalated Si/$SnSe_2$ hetero-structure.

peeling silicene sheet from $SnSe_2$ difficult which can be further confirmed with the interlayer distance. The interlayer distance between silicene and $SnSe_2$ decreases as compared to pristine hetero-structure and it is found to be 4.55 Å (d_{Si-Sn}) and 4.47 Å (d_{Si-Se}), therefore, low buckled Si atom forms chemical bond with the Se atom. The binding energy of Si/P/$SnSe_2$ is 5.934 eV and its positive value indicates that the process is exothermic. The large binding energy of P-intercalated atom compared to Cl atom shows that the interaction between hetero-structure increases. The silicene sheet slightly bends towards the $SnSe_2$ from the edge site. The above results on phosphorous interaction indicates that the Si/$SnSe_2$ is going to preserve its metallic nature. Fig. 5.8(a and b) represents the electronic band structure and PDOS of phosphorous

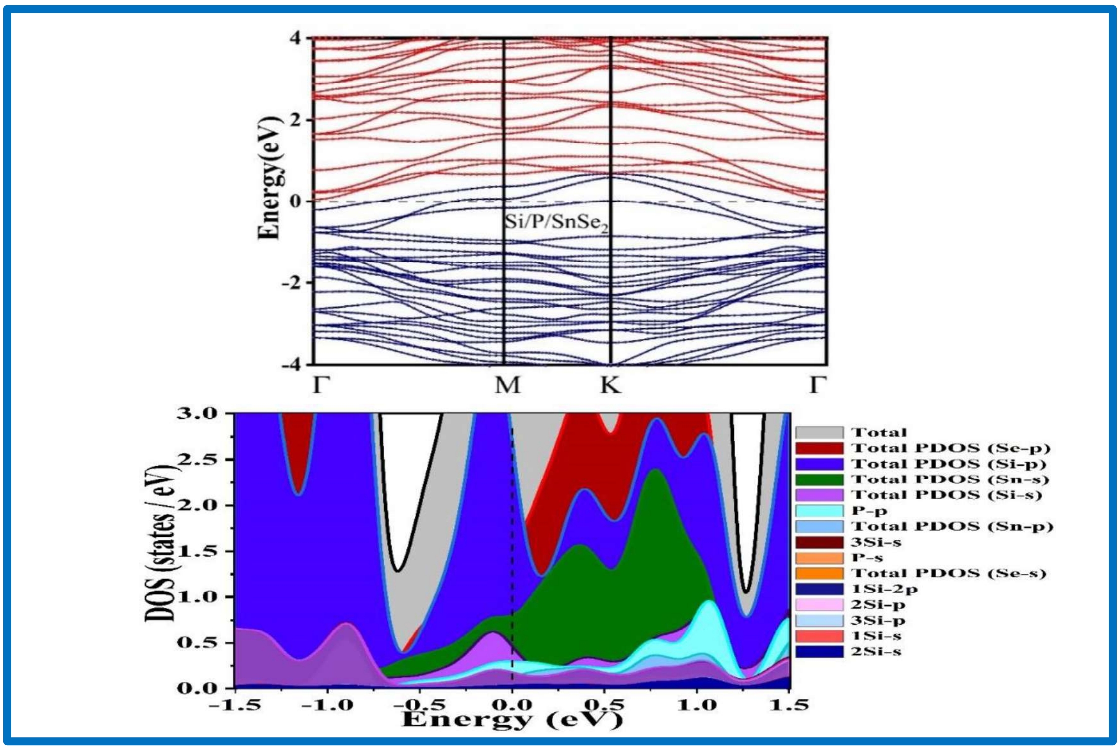

Figure 5.8: (a) The electronic bands structure and (b) partial density of state (PDOS) of Cl-intercalated Si/$SnSe_2$ hetero-structure.

intercalated Si/$SnSe_2$ hetero-structure (Si/P/$SnSe_2$) which depicts metallic nature. The metallic nature of Si/P/$SnSe_2$ is due to the overlap of p orbital of Si, Se and P with s-orbital of Si and Sn.

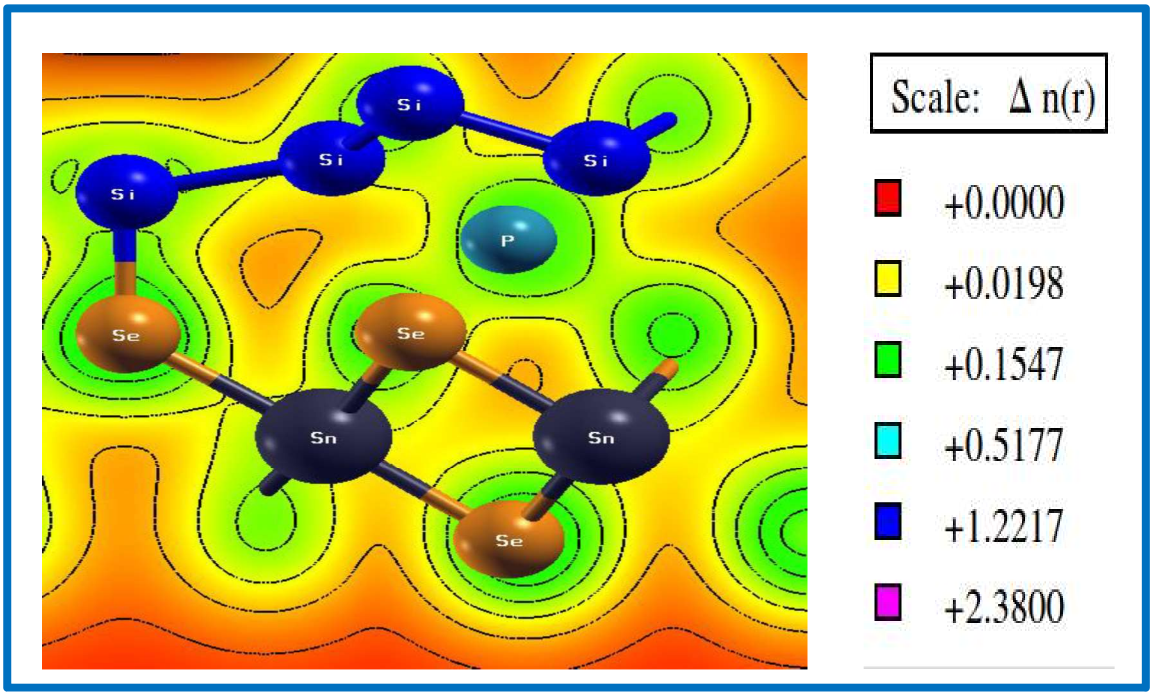

Figure 5.9: The charge density plot of P-intercalated Si/$SnSe_2$ hetero-structure.

From the charge density plot of Si/P/$SnSe_2$, we can clearly see that the charge resides at the periphery of phosphorous atoms (see Fig. 5.9). The charge density is found more between the hetero-structure compared to Si/Cl/$SnSe_2$ that shows a strong interaction between two layers which validates above results. The intercalation of phosphorus does not help to preserve the semi-metallic nature of silicene, rather it exhibits metallic nature. Above intercalated atoms are unable to avoid charge transfer due to their electronegativity whereas, the NH_3 molecule is shown to be a good intercalation molecule in previous study as it avoids charge transfer between hetero-structure. Therefore, we now turn our attention towards the properties of the system subjected to intercalation of NH_3 molecule.

5.3.2.3 Structural and electronic properties of hetero-structure (Si/SnSe₂) with intercalated ammonia (NH₃) molecule.

Intercalation of ammonia (NH_3) molecule between hetero-layers was done for two different configurations to understand its effect towards the electronic properties. In the first configuration, the hydrogen atoms face towards $SnSe_2$ layer of hetero-structure ($Si/NH_3^a/SnSe_2$) as shown in Fig. 5.10. As observed, the NH_3 molecule prefers the corner site of silicene similar to the Cl atom and shows chemisorption nature i.e. it forms bond with silicene atoms. The interlayer distance increases with the inclusion of NH_3 molecule and a significant charge transfer occurs from NH_3 molecule to silicene layer while depletion of charge is observed for $SnSe_2$

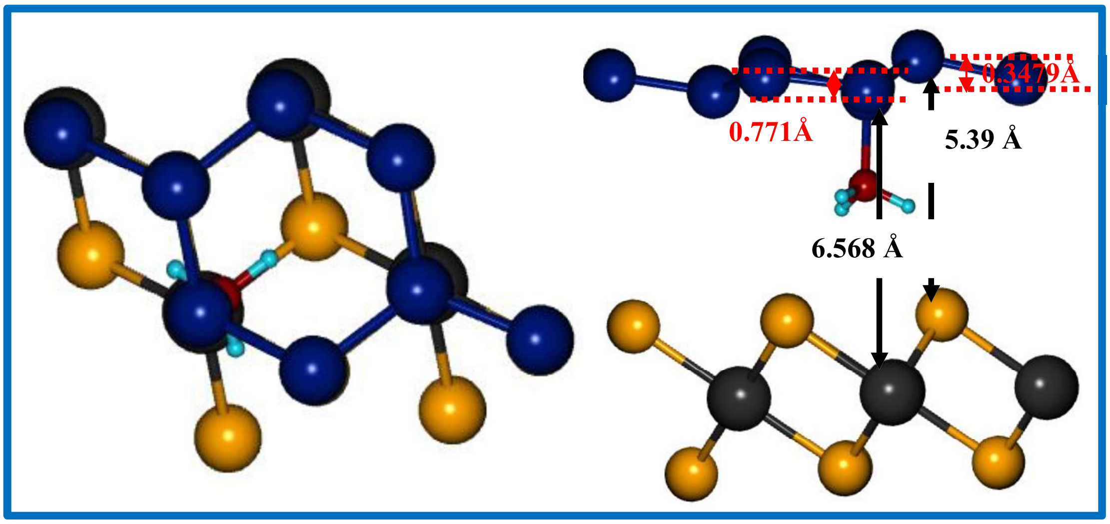

Figure 5.10*:* Top and side view of optimized structure of NH_3^a-intercalated Si/SnSe₂ hetero-structure.

layer. This can be confirmed with the charge density plot (Fig. 5.11) which clearly depicts that the charge resides near NH_3 molecule and bonded Si atoms due to strong interaction between them. The binding energy Si/NH_3^a/$SnSe_2$ is not only positive (0.75 eV) but also exhibits lower value than Cl and P intercalated hetero-structure, while it is comparable with the Si/NH_3/$PtSe_2$.[44] We have plotted electronic band structure and PDOS of Si/NH_3^a/$SnSe_2$ to explore its electronic nature and know the effect of intercalation of NH_3 molecule in deeper sense. The NH_3^a intercalated hetero-structure exhibits metallic nature similar to the Cl and P intercalated Si/$SnSe_2$. The intercalated NH_3^a molecule interacts with silicene sheet instead of $SnSe_2$ sheet. However, the nitrogen atom interacts with the silicene atoms. The electronic band structure and PDOS of Si/ NH_3^a/$SnSe_2$ depicts metallic nature (Fig. 5.12). We can see that the metallic nature

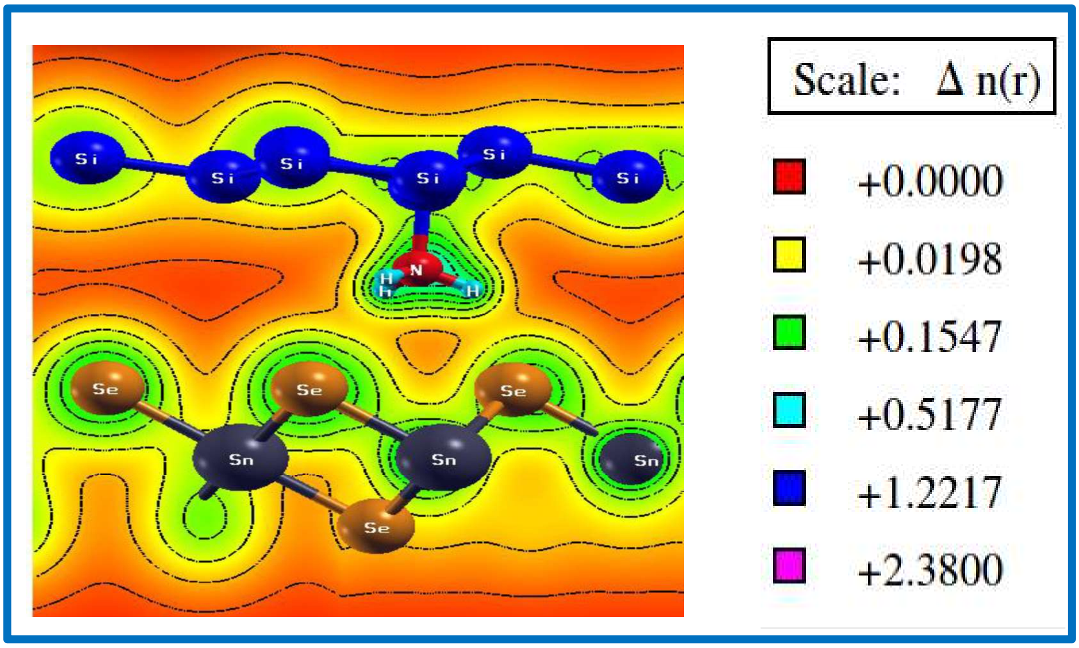

Figure 5.11: The charge density plot of NH_3^a-intercalated hetero-structure Si/$SnSe_2$.

is due to the overlap of PDOS of Si and Se atoms near Fermi level. These results show that the ammonia molecule strongly interacts with the Si atoms leading to metallic nature. In a previous report, Sattar et al.[44] have shown that the ammonia molecule interacts with $PtSe_2$ sheet leading to the band opening of silicene. In the second configuration, we kept nitrogen atom of ammonia

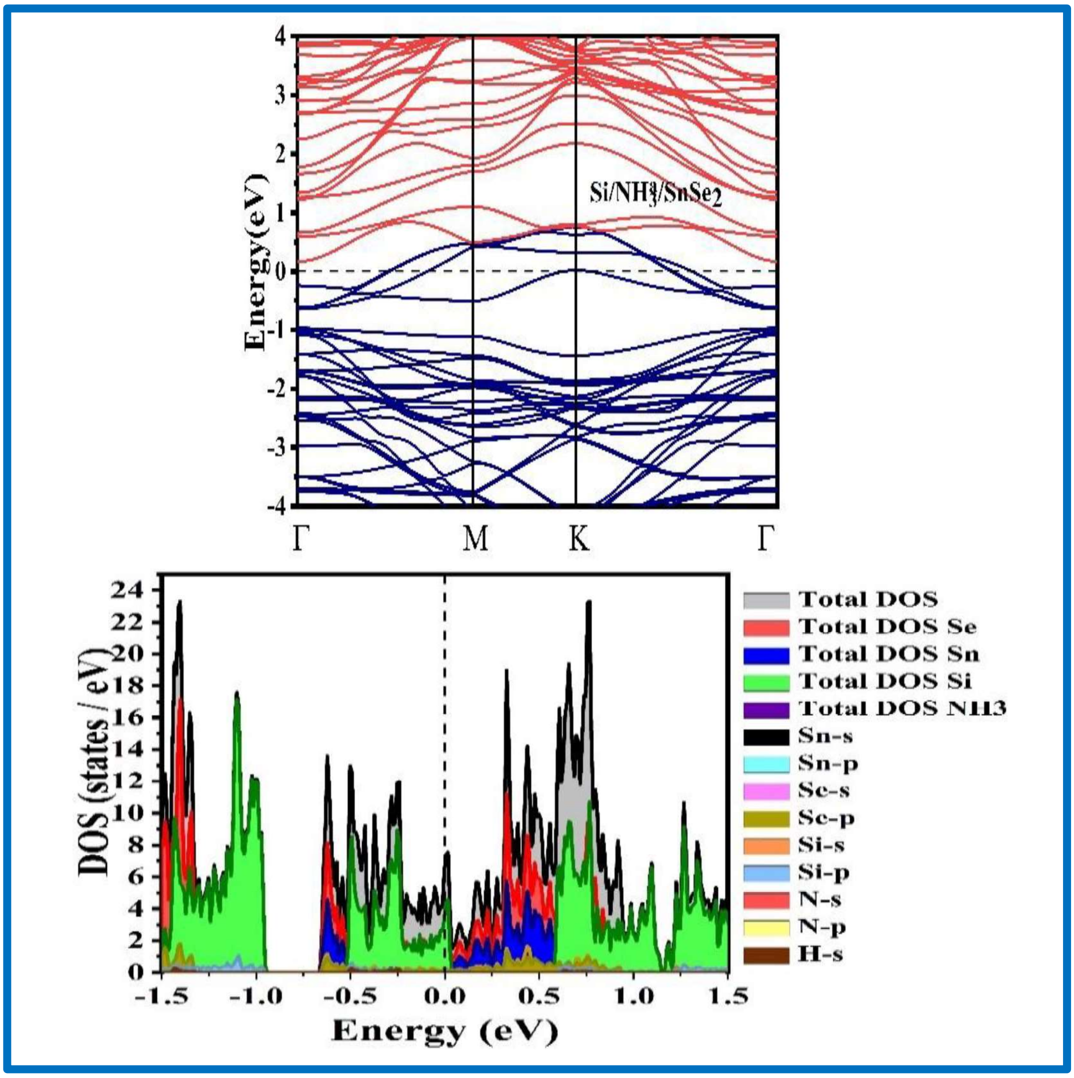

Figure 5.12: (a) The electronic bands structure and (b) partial density of state (PDOS) of NH_3^a-intercalated hetero-structure Si/SnSe2 respectively.

molecules facing towards the $SnSe_2$ (Fig. 5.13). In this case ammonia molecule preferers hollow site as compared to previous configuration. The buckling height (0.4994 Å) of silence increases by 1.5 % as compared to Si/$SnSe_2$ hetero-structure whereas, in the case of NH_3^a, it decreases due to strong interaction. Moreover, the interlayer distance increases compared to other intercalated atoms where, it is found to be 7.036 Å (d_{Si-Sn}) and 6.568 Å (d_{Si-Se}). Ammonia molecule shows physisorption nature to both the sheets. This suggests more probability of band opening or preservation of Dirac cone. To confirm physisorption of ammonia molecule, we analyzed its charge transfer and charge density plot. The depletion of charge near silicene atoms is observed compared to other ammonia configuration which shows that the charge transfer takes place from silicene atom to ammonia molecule (see Fig. 5.14). The distance between NH_3 and silicene, and

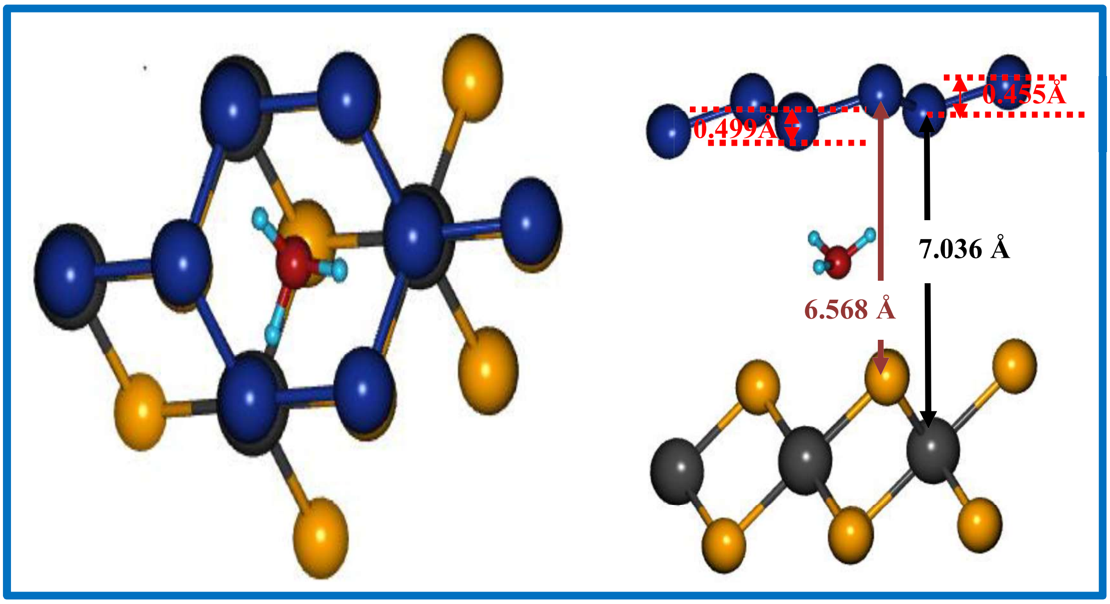

Figure 5.13*:* Top and side view of optimized structure of NH_3^b-intercalated hetero-structure Si/$SnSe_2$.

NH_3 and Se is 2.99 Å and 2.42 Å, respectively. Above results confirm physisorption nature of ammonia towards the hetero-structure. We can confirm the band opening from the electronic band structure of Si/ NH_3^b/$SnSe_2$. It exhibits semi-conducting nature with band gap of 0.23 eV (see Fig. 5.15) which is higher than $PtSe_2$ (0.153 eV).[44] Moreover, Si/ NH_3^b/$SnSe_2$ is found to be energetically more stable as compared to its counterpart configuration (Si/ NH_3^a/$SnSe_2$) and is in good agreement with previous report.[44] We have also calculated the energy required to remove the silicene sheet from the intercalated atom or molecule adsorbed substrates using Equation 5.4. The energy required is -0.266 eV, -0.204 eV, -0.143 eV and 0.004 eV for Cl, P, NH_3^a and NH_3^b, respectively. This result also shows that the interaction between hetero-structure gets weakened as we move from Cl to NH_3^b.

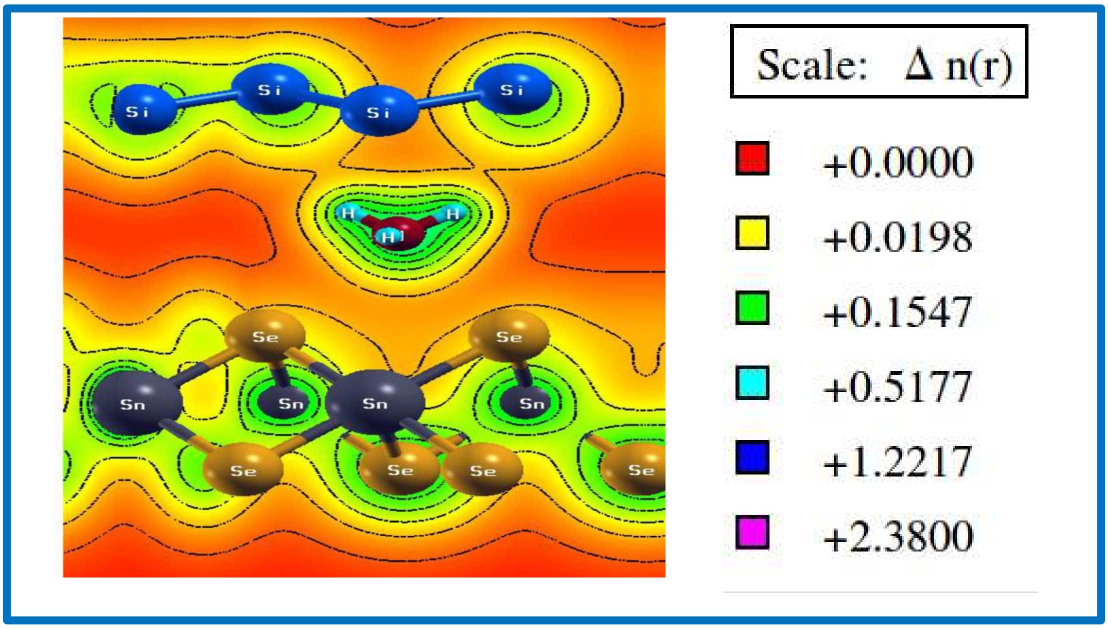

Figure 5.14*:* The charge density plot of NH_3^b-intercalated hetero-structure Si/$SnSe_2$.

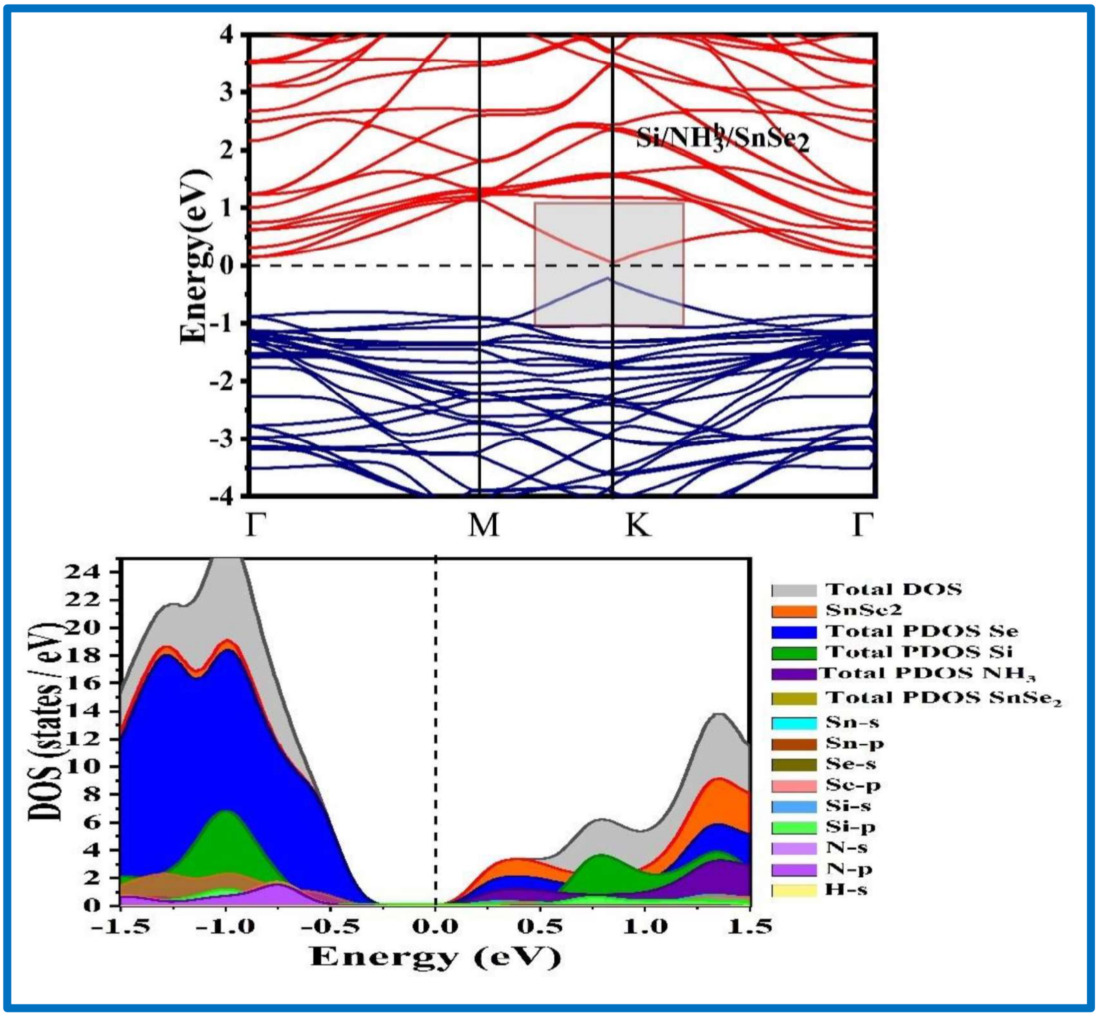

Figure 5.15: (a) The electronic bands structure and (b) partial density of state (PDOS) of NH_3^b-intercalated hetero-structure Si/SnSe$_2$ respectively.

After successful modulation of electronic properties of silicene via intercalation of ammonia molecule, we have investigated the adsorption of carbon monoxide (CO) which is considered as one of the atmospheric pollutants affecting human health. The silicene has already been used as adsorbent for adsorption of carbon monoxide.[51] The absorption of adsorbent mainly depends on the surface reactivity and interaction between them. We have analyzed charge transfer, partial density of states and binding energy to find the potential candidate as detector or absorber. We initially adsorbed CO over the silicene. Fig. 5.16 shows the optimized structure with favourable configuration of CO adsorption. We have found that the CO prefers to be in slightly tilted configuration over the hollow site of silicene sheet instead of horizontal one as compared to previous report.[51] We analyzed Lowdin charge analysis after the adsorption of CO over silicene sheet, where the charge transfer is observed from silicene to CO molecule which can be attributed to weak interaction existing between them. The distance between the Si atom of silicene and carbon atom of CO molecule is 2.62 Å that suggests physisorption nature consistent with previous report.[51] The PDOS of C and O atoms towards the anti-bond and bonding states shown in Fig. 5.17 further confirms the physisorption. The metallic nature of silicene monolayer confirms the interaction between CO_2 and silicene monolayer as a shift observed in the position of Dirac cone. These observations confirm the weak interaction between

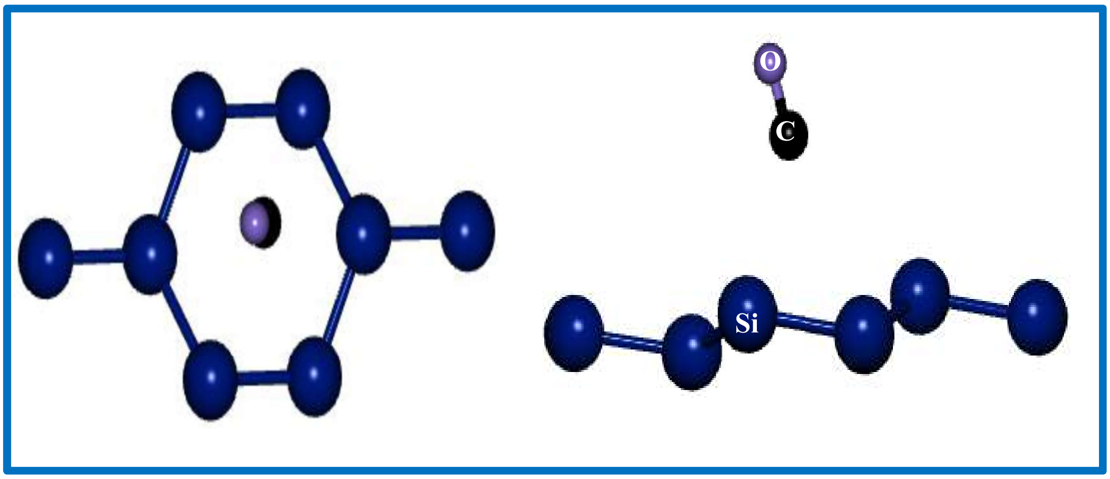

Figure 5.16: Top and side view of optimized structure of CO adsorbed over Si/SnSe$_2$.

CO and silicene monolayer. We have also calculated binding energy of CO with different substrates using equation 5.3 as follows:

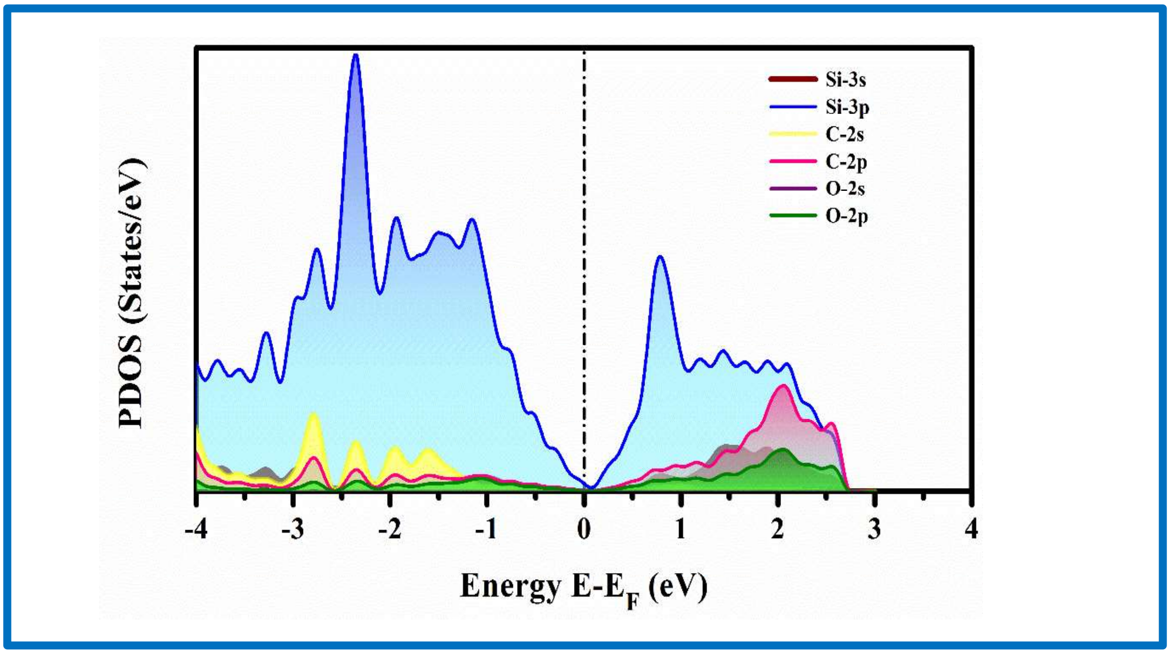

Figure 5.17: The partial density of state (PDOS) of Co adsorbed Silicene.

$$E_b = E_{tot(z-CO)} - (E_{tot(CO)} + E_{tot(z)}) \tag{5.5}$$

where, $E_{tot(z-CO)}$, $E_{tot(CO)}$ and $E_{tot(z)}$ is total energy of adsorbed CO over substrate, CO and substrate (z = silicene, SnSe$_2$, Si/P/SnSe$_2$, Si/Cl/SnSe$_2$, Si/NH$_3^a$/SnSe$_2$ and Si/NH$_3^b$/SnSe$_2$), respectively. The binding energy of CO over silicene monolayer is found to be 0.12 eV (listed in Table 5.2) where the negative sign of binding energy shows that the process is exothermic where, $E_{tot(z-CO)}$, $E_{tot(CO)}$ and $E_{tot(z)}$ is total energy of adsorbed CO over substrate, CO and substrate (z = silicene, SnSe$_2$, Si/P/SnSe$_2$, Si/Cl/SnSe$_2$, Si/NH$_3^a$/SnSe$_2$ and Si/NH$_3^b$/SnS$_2$e), respectively. The binding energy of CO over silicene monolayer is found to be 0.12 eV (listed in Table 5.2) where the negative sign of binding energy shows that the process is exothermic.

Table 5.2: Binding energy of CO molecules on adsorbent (silicene, $SnSe_2$, Si/P/$SnSe_2$, Si/Cl/$SnSe_2$, Si/NH_3^a/$SnSe_2$ and Si/NH_3^b/$SnSe_2$).

System	Binding energy (eV)	Charge transfer (e)	Distance between CO and Si (Å)
Silicene (Si)	-0.12	0.05	2.62
$SnSe_2$	-0.08	0.02	1.61(C-Se)
Si/$SnSe_2$	-0.04	0.03	3.02
Si/Cl/$SnSe_2$	-0.07	0.02	3.09
Si/P/$SnSe_2$	-0.14	0.05	2.61
Si/ NH_3^a/$SnSe_2$	-0.11	0.02	3.06
Si/ NH_3^b/$SnSe_2$	-0.06	0.019	3.12

We have adsorbed CO molecule over different adsorbents to observe its interaction. The CO molecule interacts differently with $SnSe_2$, corresponding hetero-structure and intercalated hetero-structure. Electronic properties play a vital role for the detection and binding of molecules towards adsorbent. The intercalated atoms affect electronic properties of hetero-structure as well its adsorption process. Therefore, to understand the interaction we analyzed each considered system for the adsorption of CO molecule. We observe that except silicene, CO prefers to be in parallel configuration along hollow site of the all considered adsorbents. However, the position of CO molecule is shifted as per the electronegativity of adjacent Si or Se atoms. Fig. 5.18 represents the optimized CO adsorbed over various adsorbents. Further, the carbon atom of CO molecule gets attracted towards the absorbent

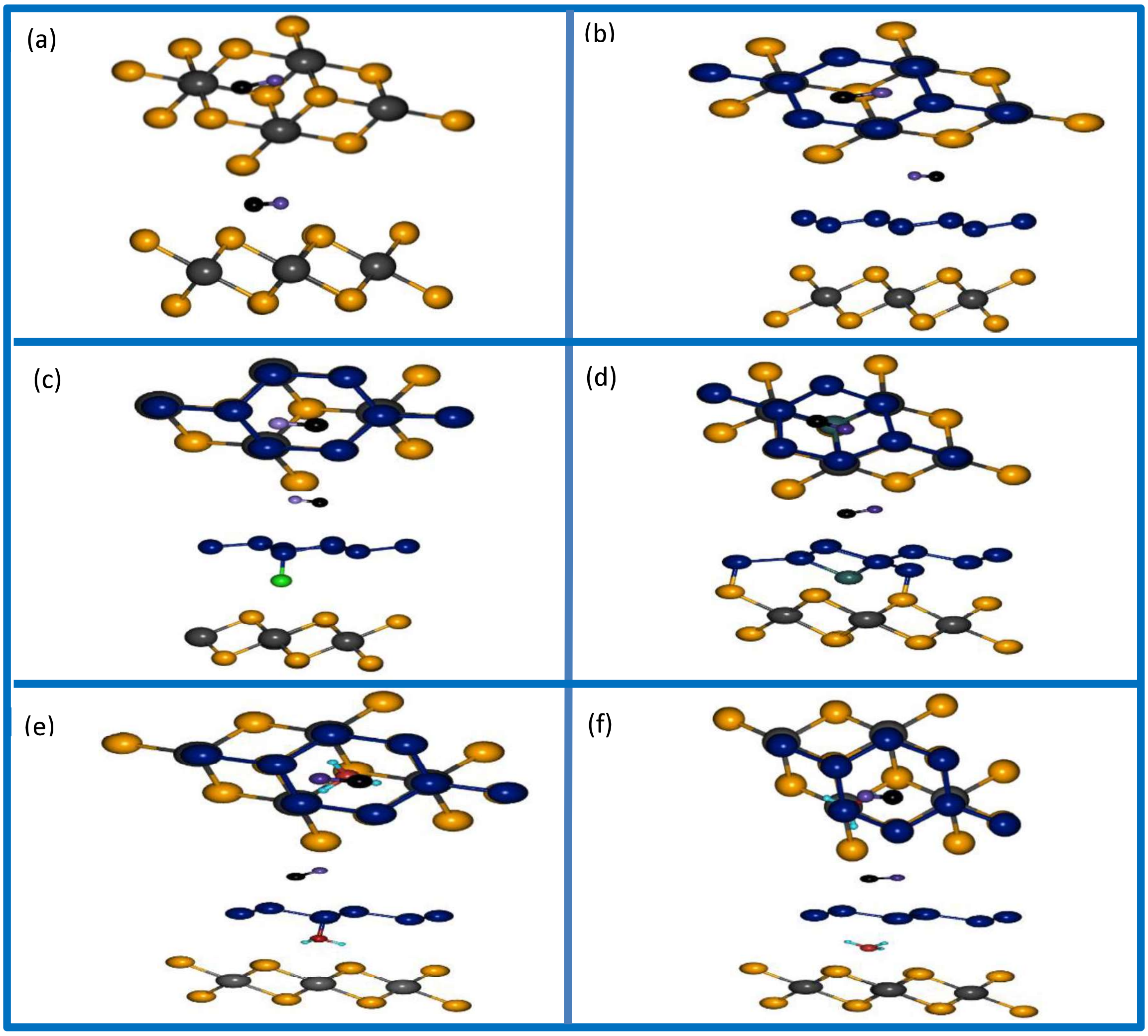

Figure 5.18*:* Top and side view of optimized structure of Co adsorbed over (a) $SnSe_2$, (b) Si/$SnSe_2$ (c) Si/Cl/$SnSe_2$ (d) Si/P/$SnSe_2$ (e)Si/NH_3^a/*$SnSe_2$ and* (f) Si/NH_3^b/*$SnSe_2$, respectively*.

whereas, oxygen atom gets repelled in the case of the intercalated hetero-structure as can be observed from Fig. 5.19(c-f). In all the cases, charge transfer from adsorbent to adsorbate is observed, and the charge transfer is about 0.2 e, 0.02 e, 0.05 e, 0.02 e and 0.019 e from $SnSe_2$, Si/$SnSe_2$, Si/Cl/$SnSe_2$, Si/P/$SnSe_2$, Si/NH_3^a/$SnSe_2$ and Si/NH_3^b/$SnSe_2$, respectively. The maximum charge transfer is observed in the case of silicene and Si/P/SnSe$_2$ and minimum charge transfer for Si/NH$_3^b$/SnSe$_2$. The distance between C atom of CO molecule and Se atom is minimum with binding energy -0.08 eV suggesting physisorption. However, the binding energy decreases in case of hetero-structure (Si/SnSe$_2$) due to strong interaction between silicene and SnSe$_2$ monolayers. The binding energy of silicene and SnSe$_2$ is higher than the hetero-structure which results in the weak adsorption of CO molecule due to strong interaction and charge transfer between them. However, intercalation of atoms or molecules weakens this interaction and tends to enhance the adsorption. Among all the intercalated hetero structure, the P

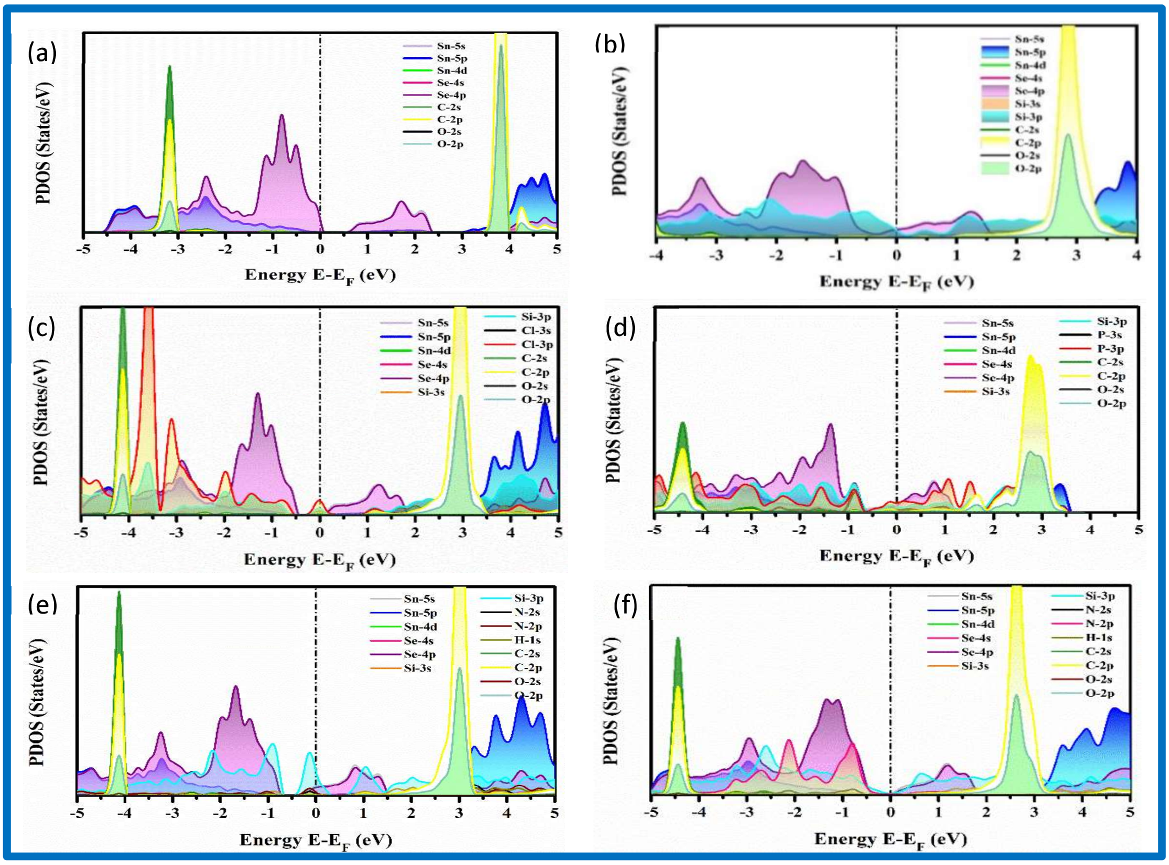

Figure 5.19*:* The partial density of state (PDOS) of Co adsorbed over (a) SnSe$_2$, (b) Si/SnSe$_2$ (c) Si/Cl/SnSe$_2$ (d) Si/P/SnSe$_2$ (e)Si/NH_3^a*/SnSe$_2$ and* (f) Si/NH_3^b*/SnSe$_2$ respectively*.

intercalated Si/$SnSe_2$ hetero-structure shows highest binding energy. In all considered adsorbents (Fig. 5.16(a-f)), the PDOS of CO molecule contributes to both anti-bonding and bonding states which validates the CO molecule physisorption nature of CO molecule. However, the contribution in the anti-bonding and bonding states varies with adsorbent. In case of $SnSe_2$ and hetero-structure, contribution of PDOS near Fermi of bonding state is lesser and symmetric whereas, the bonding state is more in case of hetero-structure compared to $SnSe_2$ and other intercalated hetero-structure. This result shows that the pristine hetero-structure weakly interacts with CO molecule as compared to another considered adsorbent. The contribution of PDOS of CO molecule in case of Si/P/$SnSe_2$ decreases, which shows that the incorporation of P atoms in hetero-structure increases its binding nature compared to pristine. In the case of Si/ NH_3^b/$SnSe_2$, we observe that the symmetry of PDOS of CO molecule in anti-bonding state gets reversed and preserves its semi-conductor nature. It is interesting to note that the absorptivity of CO molecule increases in case of metallic (Si/NH_3^a/SnSe2) as compared to its semi-conducting counterpart (Si/NH_3^b/$SnSe_2$). We found that the absorptivity of hetero-structure increases with the intercalation of molecule and thus the system can be used for sensing of CO molecule. It's less reactivity towards the CO molecule also suggests that the degradation of absorbent is less.

5.4 Conclusions

Density functional theory based *First-principles* studies have been performed to calculate the structural and electronic properties of silicene, $SnSe_2$ and Si/$SnSe_2$ hetero-structure. We found that the $SnSe_2$ strongly interacts with silicene monolayer and results an increase in buckling height by about 5.4% compared to isolated silicene. Further, our results show that the hetero-structure is energetically stable and growth of silicene on SnSe$_2$ is possible. It shows metallic nature even though buckling height and lattice mismatch are lesser compared to other di-chalcogenide substrates. The strong interaction between the monolayers can be reduced by increasing interlayer distance. The atom or molecule -intercalation within the hetero-structure not only weakens the interlayer distance but also manipulates electronic/ionic charge accumulation between the monolayers. Here, we have investigated the modulation of electronic properties of hetero-structure with the p-type dopants, phosphorous (P) and chlorine (Cl) and ammonia (NH_3). We observe that the chlorine atom gets strongly attached to the silicene monolayer due to its electron withdrawing nature. The interlayer distance in Si/SnSe$_2$ hetero-structure increases with the intercalation of Cl atom. The metallic nature of Si/Cl/SnSe$_2$ is observed due to the formation of chemical bond between Cl and Si edge atoms of silicene monolayer due to sp^3 hybridization. In the case of phosphorous intercalated Si/SnSe$_2$, we observe that the phosphorus prefers to reside on silicene than SnSe$_2$ monolayer. The phosphorus atoms form three chemical bonds with the silicon atoms of silicene due to its electronegativity and oxidation state. The interlayer distance decreases due to strong interaction and bond formation between the edge silicon atoms of silicene and Se atom of SnSe$_2$ monolayer. We observe a charge transfer from silicene monolayer to Cl and P atoms.

The ammonia molecule shows unique interaction depending on intercalation configurations. When nitrogen atom of ammonia molecule is set towards silicene sheet (Si/NH_3^a/SnSe$_2$), it prefers to be at hollow site and forms chemical bond with silicene atom resulting a charge transfer towards ammonia molecule. The interlayer distance between them gets increased but due to strong interaction between silicene and ammonia the system turns to metallic. It is interesting to note that when nitrogen of ammonia molecule faces $SnSe_2$ monolayer, there is no interaction between them and ammonia acts as an inert molecule. The strong interaction between two monolayers becomes weaker with intercalation of NH_3 in second configuration, which is energetically favorable and band opens with 0.23 eV. We conclude that the increased interlayer distance and interaction of intercalated atoms with hetero-structure weakens van der Waals interaction and tunes electronic properties of hetero-structure. The binding energy calculations show that all intercalated systems are thermodynamically stable. We adsorbed CO molecule over all considered systems to know the reactivity towards it and possible sensor application. We find that the intercalation of atoms and molecule enhances the sensing properties of the hetero-structure. In a nut-shell, a new pathway of tuning the electronic and sensing properties of 2D hetero-structures has been found by means of intercalation of monoatomic elements/small molecules, without compromising the stability of the hetero-structure. The results on tuning the structural mismatch and electronic properties of the hetero-layers serve as a guide to experimentalists for fabricating novel 2D hetero-structures and provide distinct alternatives for fine tuning of the electronic responses.

CHAPTER 5

Effect of intercalation and vertical hetero-structure Silicene/$SnSe_2$ over the electronic properties of Silicene

Reference

[1] K. Takeda and K. Shiraishi, Phys. Rev. B **50**, 14916 (1994).

[2] H. Şahin, S. Cahangirov, M. Topsakal, E. Bekaroglu, E. Akturk, R.T. Senger, and S. Ciraci, Phys. Rev. B - Condens. Matter Mater. Phys. **80**, (2009).

[3] K.S. Novoselov, A.K. Geim, S.V. Morozov, D. Jiang, Y. Zhang, S.V. Dubonos, I.V. Grigorieva, and A. Firsov, Science **306**, 666 (2004).

[4] K.S. Novoselov, D. Jiang, F. Schedin, T.J. Booth, V. V Khotkevich, S. V Morozov, and A.K. Geim, Proc. Natl. Acad. Sci. **102**, 10451 (2005).

[5] G. Le Lay, E. Salomon, and T. Angot, in 2D Mater. Prop. Devices (2017).

[6] E. Durgun, S. Tongay, and S. Ciraci, Phys. Rev. B - Condens. Matter Mater. Phys. **72**, (2005).

[7] Y. Wang, S. Zhou, J. Lu, H. Zhong, R. Quhe, C.C. Liu, Y. Yao, N. Han, Z. Yu, J. Zhao, H. Liu, and K. Wu, Prog. Mater. Sci. **83**, 24–151 (2016).

[8] L. Meng, Y. Wang, L. Zhang, S. Du, R. Wu, L. Li, Y. Zhang, G. Li, H. Zhou, W.A. Hofer, and others, Nano Lett. **13**, 685 (2013).

[9] A. Fleurence, R. Friedlein, T. Ozaki, H. Kawai, Y. Wang, and Y. Yamada-Takamura, Phys. Rev. Lett. **108**, 245501 (2012).

[10] A.J. Mannix, B. Kiraly, B.L. Fisher, M.C. Hersam, and N.P. Guisinger, ACS Nano **8**, 7538 (2014).

[11] C.L. Lin, R. Arafune, K. Kawahara, M. Kanno, N. Tsukahara, E. Minamitani, Y. Kim, M. Kawai, and N. Takagi, Phys. Rev. Lett. **110**, 76801 (2013).

[12] S. Cahangirov, H. Sahin, G. Le Lay, and A. Rubio, in Lect. Notes Phys. (2017).

[13] P. Vogt, P. De Padova, C. Quaresima, J. Avila, E. Frantzeskakis, M.C. Asensio, A. Resta, B. Ealet, and G. Le Lay, Phys. Rev. Lett. **108**, 155501 (2012).

[14] Z. Ni, H. Zhong, X. Jiang, R. Quhe, G. Luo, Y. Wang, M. Ye, J. Yang, J. Shi, and J. Lu, Nanoscale **6**, 7609 (2014).

[15] C.C. Liu, W. Feng, and Y. Yao, Phys. Rev. Lett. **107**, 076802 (2011).

[16] A. Molle, J. Goldberger, M. Houssa, Y. Xu, S.-C. Zhang, and D. Akinwande, Nat. Mater. **16**, 163 (2017).

[17] K. Yang, S. Cahangirov, A. Cantarero, A. Rubio, and R. D'Agosta, Phys. Rev. B - Condens. Matter Mater. Phys. **89**, 125403 (2014).

[18] H. Sadeghi, S. Sangtarash, and C.J. Lambert, Sci. Rep. **6**, 1176 (2015).

[19] R. Chandiramouli, A. Srivastava, and V. Nagarajan, Appl. Surf. Sci. **351,** 662 (2015).

[20] E.H. Song, S.H. Yoo, J.J. Kim, S.W. Lai, Q. Jiang, and S.O. Cho, Phys. Chem. Chem. Phys. **16**, 23985 (2014).

[21] D. Kaltsas, L. Tsetseris, and A. Dimoulas, J. Phys. Condens. Matter **24**, 442001 (2012).

[22] Y.P. Wang and H.P. Cheng, Phys. Rev. B - Condens. Matter Mater. Phys. **87**, 1 (2013).

[23] G. Giovannetti, P.A. Khomyakov, G. Brocks, V.M. Karpan, J. Van Den Brink, and P.J. Kelly, Phys. Rev. Lett. **101**, 178 (2008).

[24] P.A. Khomyakov, G. Giovannetti, P.C. Rusu, G. Brocks, J. Van Den Brink, and P.J. Kelly, Phys. Rev. B - Condens. Matter Mater. Phys. **79**, 195425 (2009).

[25] J. Wintterlin and M.L. Bocquet, Surf. Sci. **603**, 1841 (2009).

[26] J. Zheng, Y. Wang, L. Wang, R. Quhe, Z. Ni, W.N. Mei, Z. Gao, D. Yu, J. Shi, and J. Lu, Sci. Rep. 3, 2081 (2013).

[27] Z. Xu and M.J. Buehler, J. Phys. Condens. Matter **22**, 485301 (2010).

[28] F. Giubileo and A. Di Bartolomeo, Prog. Surf. Sci. **92,** 143 (2017).

[29] R. Quhe, Y. Yuan, J. Zheng, Y. Wang, Z. Ni, J. Shi, D. Yu, J. Yang, and J. Lu, Sci. Rep. **4**, 31 (2014).

[30] Y. Cai, C.P. Chuu, C.M. Wei, and M.Y. Chou, Phys. Rev. B - Condens. Matter Mater. Phys. **88**, 245408 (2013).

[31] M. Houssa, G. Pourtois, V. V. Afanas'Ev, and A. Stesmans, Appl. Phys. Lett. **96**, 082111 (2010).

[32] T.P. Kaloni and U. Schwingenschlögl, J. Appl. Phys. **583**, 137(2013).

[33] S. Kokott, P. Pflugradt, L. Matthes, and F. Bechstedt, J. Phys. Condens. Matter **26**, 185002. (2014).

[34] N. Gao, J.C. Li, and Q. Jiang, Phys. Chem. Chem. Phys. **16**, 11673 (2014).

[35] A. Bhattacharya, S. Bhattacharya, and G.P. Das, Appl. Phys. Lett. **114**, 10297 (2013).

[36] D. Chiappe, E. Scalise, E. Cinquanta, C. Grazianetti, B. Van Den Broek, M. Fanciulli, M. Houssa, and A. Molle, Adv. Mater. **26**, 2096 (2014).

[37] Y. Ding and Y. Wang, Appl. Phys. Lett. **103**, 43114 (2013).

[38] M.X. Chen, Z. Zhong, and M. Weinert, Phys. Rev. B **94**, 075409 (2016).

[39] L. Li and M. Zhao, J. Phys. Chem. C (2014).

[40] E. Scalise, M. Houssa, E. Cinquanta, C. Grazianetti, B. Van Den Broek, G. Pourtois, A. Stesmans, M. Fanciulli, and A. Molle, 2D Mater. **1,** 011010 (2014).

[41] E. Scalise and M. Houssa, Nano Res. **10**, 1697 (2017).

[42] E. Cinquanta, E. Scalise, D. Chiappe, C. Grazianetti, B. Van Den Broek, M. Houssa, M. Fanciulli, and A. Molle, J. Phys. Chem. **117**, 16719 (2013).

[43] E. Scalise, K. Iordanidou, V. V. Afanas'ev, A. Stesmans, and M. Houssa, Nano Res. **11**, 1169 (2018).

[44] S. Sattar, N. Singh, and U. Schwingenschlögl, ACS Appl. Mater. Interfaces **10**, 4266 (2018).

[45] D. Sung, G. Kim, and S. Hong, Sci. Rep. **9**, 3623 (2019).

[46] J.P. Perdew and K. Burke, Phys. Rev. B **54**, 16533 (1996).

[47] W. Kohn and L.J. Sham, Phys. Rev. (1965).

[48] P. Giannozzi, S. Baroni, N. Bonini, M. Calandra, R. Car, C. Cavazzoni, D. Ceresoli, G.L. Chiarotti, M. Cococcioni, I. Dabo, A. Dal Corso, S. De Gironcoli, S. Fabris, G. Fratesi, R. Gebauer, U. Gerstmann, C. Gougoussis, A. Kokalj, M. Lazzeri, L. Martin-Samos, N. Marzari, F. Mauri, R. Mazzarello, S. Paolini, A. Pasquarello, L. Paulatto, C. Sbraccia, S. Scandolo, G. Sclauzero, A.P. Seitsonen, A. Smogunov, P. Umari, and R.M. Wentzcovitch, J. Phys. Condens. Matter **21**, 395502 (2009).

[49] H. Monkhorst and J. Pack, Phys. Rev. B **13**, 5188 (1976).

[50] S. Grimme, J. Comput. Chem. **30**, 1787 (2006).

[51] M.R. Al Fauzan, W.D. Astuti, G. Al Fauzan, and S. Sholihun, Molekul **13**, 92 (2018).